

Jet quenching from heavy to light ion collisions

B.G. Zakharov^{1,2}

¹*L.D. Landau Institute for Theoretical Physics, GSP-1, 117940, Kosygina Str. 2, 117334 Moscow, Russia*

²*Steklov Mathematical Institute, Russian Academy of Sciences, Gubkin str. 8, 119991 Moscow, Russia*

E-mail: bgz@itp.ac.ru

ABSTRACT: We perform an analysis of jet quenching in heavy and light ion collisions for scenarios without and with quark-gluon plasma formation in pp collisions. We find that the results for these scenarios are very similar, and both of them are in reasonable agreement with data for heavy ion collisions. However, their results become differ significantly for light nuclei. Using the parameters fitted to heavy ion data on the nuclear modification factor R_{AA} , we make predictions for 0.2 and 7 TeV O+O collisions that can be verified by future experiments at RHIC and the LHC.

Contents

1	Introduction	1
2	Basic aspects of the jet quenching scheme	5
3	Models of the QGP fireballs for AA and pp collisions	9
3.1	The QGP fireball in AA collisions	10
3.2	The mQGP fireball parameters for pp collisions	12
4	Numerical results	14
4.1	Optimal κ from the χ^2 fit	14
4.2	Predictions for R_{pp} , R_{AA} and azimuthal asymmetry v_2	15
4.3	Jet quenching in pA collisions	24
5	Conclusions	25

1 Introduction

It is believed that heavy ion collisions at the RHIC and LHC energies produce a deconfined quark-gluon plasma (QGP). Strong suppression of the high- p_T particles observed in heavy ion collisions (usually called jet quenching) at RHIC and the LHC is one of the major signals of the QGP formation. This phenomenon is a consequence of parton energy loss in the QGP. For fast partons the energy loss is dominated by the radiative mechanism through induced gluon emission [1–6]. The suppression of particle spectra in AA collisions is quantified by the nuclear modification factor R_{AA} . For a given centrality bin Δc (which is experimentally determined via charged hadron multiplicities) R_{AA} is defined as the ratio of particle yield in AA collisions to that in pp collisions scaled with the number of binary collisions

$$R_{AA} = \frac{d^2 N_{AA}/dp_T^2 dy}{N_{ev} \langle T_{AA} \rangle_{\Delta c} d^2 \sigma_{pp}/dp_T^2 dy}, \quad (1.1)$$

where $\langle T_{AA} \rangle_{\Delta c}$ is the nuclear overlap function for centrality class Δc . The relation between centrality c and the impact parameter b of AA collision is usually defined within the Glauber model. Theoretical calculations of the nuclear suppression are commonly performed assuming that the medium jet modification occurs only in AA collisions, and is absent in pp collisions, i.e., the pp yield in the denominator on the righthand side of (1.1) can be calculated in the standard pQCD approach. In

this scenario, with the Glauber initial conditions for the QGP fireball at the proper time $\tau_0 \sim 0.5$ fm, one can obtain within pQCD jet quenching models rather good description of the available data on the nuclear modification factor from RHIC for Au+Au collisions and from LHC for Pb+Pb and Xe+Xe collisions (see, e.g., Refs. [7–11]). However, it is possible that the assumption that QGP is not formed in pp collisions is not valid. The observation of the ridge effect in high-multiplicity pp collisions at the LHC [12] (and even in lower-multiplicity pp collisions [13]), suggests that a small size QGP fireball can be created in pp collisions as well, because the hydrodynamic transverse flow seems to be the most natural explanation for the ridge effect. But an alternative interpretation of the ridge phenomenon via the initial state effects [14], without the collective flow in the final state, is not excluded. The formation of the QGP droplets in collisions of small systems is now one of the challenging issues for high energy QCD. Future experiments on light ion collisions at RHIC [15] and at the LHC [16–18] will allow to understand better the role of the collective effects in small systems.

In the case of a mini-QGP (mQGP) formation in pp collisions, even if it occurs only in a part of jet events, the parton shower and the inclusive pp cross section will be affected by the parton energy loss in the mQGP. It is important that the jet events in pp collisions have favorable conditions for QGP formation, as compared to the minimum bias events, since the charged multiplicity density of the soft (underlying-event (UE)) hadrons in the jet events, $dN_{ch}^{ue}/d\eta$, turns out to be bigger than the ordinary minimum bias multiplicity density by a factor (we denote it as K_{ue}) of $\sim 2 - 2.5$ [19]. The K_{ue} grows with momentum of the leading charged jet hadron at $p_T \lesssim 3 - 5$ GeV, and then flattens out [20–24]. The enhancement of the UE multiplicity may be due to the fact that jet production should be most probable for central pp collisions, and due to the initial state radiation that accompanies hard jet production. For the LHC energies $dN_{ch}^{ue}/d\eta$ at $\eta \sim 0$ turns out to be larger than the critical pseudorapidity density $dN_{ch}/d\eta \sim 6$ for beginning of the regime with formation of the hot QCD matter in pp collisions found in [25] from variation of the average transverse hadron momentum $\langle p_T \rangle$ with $dN_{ch}/d\eta$, and than a more conservative value $dN_{ch}/d\eta \sim 9$ obtained in [26]¹. The onset of the regime with QGP formation at $dN_{ch}/d\eta \gtrsim 5 - 10$ is also supported by the observation of a steep growth of the strange particle production in pp collisions in the range $dN_{ch}/d\eta \sim 2 - 8$ [27]. For pp collisions at the RHIC energy $\sqrt{s} = 0.2$ TeV $dN_{ch}^{ue}/d\eta \sim 6$. Thus, one can expect for the UEs in jet production in pp collisions at RHIC energies the thermalization may be incomplete. Of course, the transition to the regime of a thermalized QCD matter may be smooth. It is possible that at the beginning the final state interactions in the parton system are weak and lead only to a small

¹We make a reasonable assumption that for $dN_{ch}^{ue}/d\eta$ equal to $dN_{ch}/d\eta$ dynamics of the UE soft hadron production in pp jet events is similar to that for pp collisions without jet detecting.

modification of the free-stream evolution [28]. Also, it is clear that, due to event-by-event fluctuations of the entropy/energy production, the QGP can be formed in some part of jet events even for a small average UE multiplicity density at $\sqrt{s} = 0.2$ TeV. Therefore, some medium jet modification in pp collisions may already occur at the RHIC energies.

In the presence of the mQGP, the real inclusive pp cross section is determined by the product of the pQCD cross section and the medium modification factor R_{pp} (which accounts for the jet final state interaction in the mQGP)

$$d\sigma(pp \rightarrow hX)/d\mathbf{p}_T dy = R_{pp} d\sigma_{pert}(pp \rightarrow hX)/d\mathbf{p}_T dy. \quad (1.2)$$

The first pQCD calculations of R_{pp} have been performed in [29, 30] within the light-cone path integral (LCPI) approach [3] to induced gluon emission, using the measured UE charged multiplicity density for calculation of the initial mQGP temperature. The results of [30] show that for pp collisions at the LHC energies medium suppression of hadron spectra can be $\sim 20 - 30\%$ at $p_T \sim 10 - 20$ GeV. Since R_{pp} is rather close to unity and has a smooth p_T -dependence it is difficult to differentiate the scenarios with and without medium suppression using only data on the high- p_T hadron spectra in pp collisions. In [29] it was suggested to use as a signal of jet quenching in pp collisions variation of the photon/hadron-tagged jet fragmentation functions (FFs) with the UE multiplicity. The recent preliminary data from ALICE [31] on the jet FF modification factor I_{pp} at $\sqrt{s} = 5.02$ TeV for the hadron-tagged jets (with the trigger hadron momentum $8 < p_T < 15$ GeV, and the associated away side hadron momentum in the range $4 < p_T < 6$ GeV) show a monotonic decrease of I_{pp} with the UE multiplicity by about 20% for the UE multiplicity density range $\sim 5 - 20$. This agrees qualitatively with predictions of [29]. The observation of decrease of I_{pp} with the UE multiplicity, if confirmed, will be a strong argument for the scenario with mQGP formation in pp jet events.

Evidently, for the scenario with mQGP formation in pp collisions the theoretical R_{AA} , which corresponds to the experimentally measured R_{AA} , given by (1.1), reads

$$R_{AA} = R_{AA}^{st}/R_{pp}, \quad (1.3)$$

where R_{AA}^{st} is the standard nuclear modification factor calculated with the pQCD pp cross section. For a weak jet quenching in the mQGP, i.e., for R_{pp} close to unity, observation of the effect of the $1/R_{pp}$ factor in (1.3) from comparison with data on R_{AA} for heavy nuclei, when $R_{AA} \sim 0.15 - 0.5$, is a hopeless task, because uncertainties of the present theoretical jet quenching models are rather large and the presence of $1/R_{pp}$ in (1.3) may be mimicked by changes of the parameter values. However, the effect from $1/R_{pp}$ factor can become more pronounced in the case of collisions of light nuclei, when R_{AA}^{st} also becomes close to unity. This could potentially be verified by the future planned experimental study of jet quenching for oxygen-oxygen collisions

at RHIC ($\sqrt{s} = 0.2$ TeV) [15] and at the LHC [17, 18] ($\sqrt{s} = 7$ TeV). In light of this, it is highly desirable to perform a quantitative analysis of jet quenching in O+O collisions at the RHIC and LHC energies for scenarios with and without mQGP formation in pp collisions.

In the present work, by fixing free parameters from fitting available data on R_{AA} for heavy ion collisions, we perform calculations of the nuclear modification factor for 0.2 and 7 TeV O+O collisions for scenarios with and without mQGP formation in pp collisions (we will often omit for clarity adding “in pp collisions”), and for an intermediate scenario when mQGP is formed only in pp collisions at the LHC energies. We use the jet quenching model of [32] (with some improvements made in [11]), based on the LCPI approach [3] to induced gluon emission. We perform calculations of the radiative energy loss using the method suggested in [33], which allows to account for accurately the Coulomb effects in multiple parton scattering. An important feature of our calculations is that we use a temperature dependent parametrization of the running α_s (suggested in [34]). In [34] it was demonstrated that the T -dependent QCD coupling largely solves the problem of difference between the optimal values of α_s for the RHIC and LHC energies [11, 35]. Use of the T -dependent QCD coupling allows to avoid the ambiguities for small systems (pp and light ion collisions) connected with the choice of α_s for large and small size QGP, because the parameters, fitted to data for heavy ion collisions, automatically fix α_s for small size QGP. This improves the reliability of the results, as compared to our previous analyses of jet quenching in pp collisions [29, 30, 36]. There we used a unique α_s , which does not depend on the local QGP temperature. The disadvantage of this ansatz is that it leaves ambiguous how to choose α_s for the mQGP fireball in pp collisions. Note that the issue of jet quenching in light ion collisions was addressed recently in [10] within the BDMPS formalism [2] describing multiple parton scattering in terms of the transport coefficient \hat{q} . However, the scenario with mQGP formation was not considered in [10].

The plan of the paper is as follows. In Sec. 2, we briefly review the theoretical framework. In Sec. 3, we discuss the models of the QGP fireballs in AA and in pp collisions used in our jet quenching calculations. In Sec. 4 we first perform the χ^2 fit of the experimental data from the LHC on R_{AA} for Pb+Pb and Xe+Xe collisions for determining the optimal free parameters. Then, we present results for R_{pp} and R_{AA} and for the elliptic flow coefficient v_2 for heavy ion and for O+O collisions obtained with the optimal free parameters for scenarios without and with mQGP formation. We conclude with a brief discussion of jet quenching in pA collisions. Conclusions are contained in Sec. 5.

2 Basic aspects of the jet quenching scheme

Our theoretical scheme for calculation of the medium modification factors is similar to the one used in our previous jet quenching analyses (see [11, 30, 32, 34]). For this reason, here we only outline its main aspects. For AA collisions we write the nuclear modification factor R_{AA}^{st} for given impact parameter b (we consider the midrapidity region around $y = 0$)

$$R_{AA}^{st}(b, \mathbf{p}_T, y) = \frac{dN(A + A \rightarrow h + X)/d\mathbf{p}_T dy}{T_{AA}(b)d\sigma(p + p \rightarrow h + X)/d\mathbf{p}_T dy}, \quad (2.1)$$

where $T_{AA}(b) = \int d\boldsymbol{\rho} T_A(\boldsymbol{\rho}) T_A(\boldsymbol{\rho} - \mathbf{b})$ is the nuclear profile function, $T_A(\boldsymbol{\rho}) = \int dz \rho_A(\sqrt{\rho^2 + z^2})$ is the nuclear thickness function (with ρ_A the nuclear density). The differential yield of the process $A + A \rightarrow h + X$ in the nominator on the righthand side of (2.1) reads

$$\frac{dN(A + A \rightarrow h + X)}{d\mathbf{p}_T dy} = \int d\boldsymbol{\rho} T_A(\boldsymbol{\rho} + \mathbf{b}/2) T_A(\boldsymbol{\rho} - \mathbf{b}/2) \frac{d\sigma_m(N + N \rightarrow h + X)}{d\mathbf{p}_T dy}, \quad (2.2)$$

where $d\sigma_m/d\mathbf{p}_T dy$ is the medium-modified cross section, given by

$$\frac{d\sigma_m(N + N \rightarrow h + X)}{d\mathbf{p}_T dy} = \sum_i \int_0^1 \frac{dz}{z^2} D_{h/i}^m(z, Q) \frac{d\sigma(N + N \rightarrow i + X)}{d\mathbf{p}_T^i dy}. \quad (2.3)$$

Here $\mathbf{p}_T^i = \mathbf{p}_T/z$ is the transverse momentum of the initial hard parton, $d\sigma(N + N \rightarrow i + X)/d\mathbf{p}_T^i dy$ is the ordinary pQCD hard cross section, and $D_{h/i}^m(z, Q)$ is the medium-modified FF for transition of the initial hard parton i , with virtuality $Q \sim p_T^i$, to the final hadron h . The FF $D_{h/i}^m$ can symbolically be written as the triple z -convolution

$$D_{h/i}^m(Q) \approx D_{h/j}(Q_0) \otimes D_{j/k}^{in} \otimes D_{k/i}^{DGLAP}(Q), \quad (2.4)$$

where $D_{k/i}^{DGLAP}$ is the DGLAP parton FF for $i \rightarrow k$ transition, $D_{j/k}^{in}$ describes the in-medium $j \rightarrow k$ transition due to induced gluon emission, and $D_{h/j}$ is the ordinary vacuum FF for transition of the parton j to the final hadron h . For $D_{h/j}(z, Q_0)$ we use the KKP [37] parametrization with $Q_0 = 2$ GeV. We compute the DGLAP FFs $D_{k/i}^{DGLAP}$ with the help of the PYTHIA event generator [38].

The main ingredient in our analysis is the FF $D_{j/k}^{in}$, which describes the medium effects. We evaluate $D_{j/k}^{in}$ via the induced gluon spectrum dP/dx (x is the gluon fractional momentum) in the approximation of independent gluon emission [39]. A detailed description of the method for evaluation of the induced gluon spectrum within the LCPI formalism and the implementation of the approximation of independent gluon emission for calculation of $D_{j/k}^{in}$ can be found in [11, 40].

The induced gluon spectrum dP/dx depends on the QGP fireball density/temperature profile along the jet trajectory. Since the QGP temperature depends crucially on the size of the collision system, for a joint analysis of jet modification for large and small

size collision systems it is important to account for the temperature dependence of the in-medium QCD coupling. In the present analysis we calculate the gluon induced spectrum for running temperature dependent α_s . As in [34], we use the parametrization of $\alpha_s(Q, T)$ in the form

$$\alpha_s(Q, T) = \begin{cases} \frac{4\pi}{9 \log(Q^2/\Lambda_{QCD}^2)} & \text{if } Q > Q_{fr}(T) , \\ \alpha_s^{fr}(T) & \text{if } Q_{fr}(T) \geq Q \geq cQ_{fr}(T) , \\ \alpha_s^{fr}(T) \times (Q/cQ_{fr}(T)) & \text{if } Q < cQ_{fr}(T) , \end{cases} \quad (2.5)$$

where $Q_{fr}(T) = \Lambda_{QCD} \exp\{2\pi/9\alpha_s^{fr}(T)\}$ (in the present analysis we take $\Lambda_{QCD} = 200$ MeV). We perform calculations for $c = 0.8$ and $c = 0$. We take $Q_{fr} = \kappa T$, and perform fit of the free parameter κ using data on the nuclear modification factor R_{AA} for heavy ion collisions. The parametrization (2.5) with nonzero c is supported by the lattice results for the in-medium α_s in the coordinate space via calculation of the free energy of a static heavy quark-antiquark pair [41]. The results of [41] give $\alpha_s(r, T)$ that becomes close to the ordinary vacuum QCD coupling $\alpha_s(Q)$ with $Q \sim 1/r$ at $r \ll 1/T$. In the infrared region it reaches maximum at $r \sim 1/\kappa T$ with $\kappa \sim 4$, and then it falls to zero. With identification $r \sim 1/Q$, this behavior is similar to that obtained in the momentum representation within the functional renormalization group [42]. The choice $c = 0$ is similar to the model with α_s frozen in the infrared region [43, 44]. Details of incorporating the T -dependence of α_s into the LCPI scheme can be found in [34]. It should be emphasized that the use of the running α_s is very important in dealing with jet quenching simultaneously in a large size QGP for heavy ion collisions and in a smaller QGP for light ion and pp collisions, because the typical virtuality in induced gluon emission increases with decreasing medium size. The growth of the virtuality scale from heavy ion to pp collisions turns out to be quite large (by a factor of ~ 2 [30]).

We calculate the induced gluon spectrum with the Debye mass obtained in the lattice analysis [45], and take $m_q = 300$ and $m_g = 400$ MeV for the light quark and gluon quasiparticle masses in the QGP [46]. In numerical calculations for the T -dependence of the Debye mass (and of $\alpha_s(Q, T)$) we define the temperature via the lattice entropy density $s(\tau)$ obtained in [47]. For a given fireball entropy, this procedure gives T which is somewhat larger than the ideal gas temperature.

For evaluation of R_{AA} for a given centrality range Δc , we perform accurate averaging over the geometry of AA collision and over the jet trajectories in the medium. As in [32] we performed calculations for a QGP fireball with a uniform density distribution in the transverse plane, and with the Bjorken 1+1D longitudinal expansion [48]. The approximation of a uniform fireball is a crucial simplification, because in this case the medium density profile along the fast parton trajectory is independent of the jet production point (only its length L varies). This approximation greatly

reduces the computational time, since we can first tabulate the L -dependence of the induced gluon spectrum, and then to use it in computations of the FFs for arbitrary geometry of the jet production.

We evaluate the medium modification factor R_{pp} for pp collisions in a similar way. However, for pp collisions we need only the medium modification factor for the whole range of the impact parameter. The azimuthal dependence of jet quenching in mQGP is irrelevant for calculation of R_{pp} . Therefore, averaging over the geometry of the pp collision is simply reduced to averaging of the medium modified FFs over the parton path length L in the medium. We perform averaging over L for a symmetric fireball of radius R_f produced in the central pp collision. This procedure seems to be reasonable, since the jet production should be dominated by the head-on collisions, and the azimuthal asymmetry is anyway irrelevant for R_{pp} . We evaluate the L -distribution using the MIT bag model quark density (we assume that quarks and gluons have similar distributions in the transverse coordinates). The L -distribution turns out to be strongly peaked around $L \sim R_f$. For this reason the L -fluctuations lead to a small change of R_{pp} as compared to the R_{pp} calculated for $L = R_f$.

As in our previous jet quenching analyses, we calculate the parton hard cross sections in the LO pQCD with the CTEQ6 [49] parton distribution functions. For nuclei we use the nuclear parton distributions with the EPS09 correction [50]. To simulate the higher order effects we take for the virtuality scale in α_s the value aQ with $a = 0.265$ (as in the PYTHIA event generator [38]). This gives for pp collisions a fairly good description of the p_T -dependence of the hadron spectra for the scenario without mQGP formation. In principle, for scenario with mQGP formation in pp collisions the perturbative cross section in formula (1.2) should differ from that for the scenario without jet quenching due to presence of R_{pp} on the righthand side of (1.3). For a fully consistent treatment of R_{pp} one should use a bootstrap procedure with adjusting the free parameters to fit the experimental pp cross section. However, this consistent procedure does not make much sense (at least at this stage). The point is that the hadron spectra have a very steep p_T -dependence (as compared to a weak p_T -dependence of R_{pp}). For this reason R_{pp} (and R_{AA}) is only weakly sensitive to possible difference in the perturbative cross sections for scenarios without and with jet quenching in pp collisions. To roughly mimic the change of the pQCD pp cross section in scenario with mQGP, we performed calculations of R_{pp} and R_{AA} using for the α_s virtuality scale in the hard cross sections $a'Q$ with $a' = 0.13$ for the LHC energies and $a' = 0.205$ for the RHIC energy $\sqrt{s} = 0.2$ TeV. These values of a' give the p_T -dependence of the righthand side of (1.2) which is reasonably close to that for perturbative cross section without jet quenching for the hard scale aQ with the PYTHIA prescription $a = 0.265$ (which we use for scenario without mQGP formation). However, we have found that the effect of the modification of the hard cross section for the mQGP version on our predictions for R_{pp} and R_{AA} is very small, as expected.

As in [32], we treat the effect of the collisional energy loss, which is relatively small [51–53], as a small perturbation to the radiative jet quenching. We incorporate it in calculating the FFs $D_{j/k}^{in}$ by renormalizing the initial QGP temperature according to the relation

$$\Delta E_{rad}(T_0') = \Delta E_{rad}(T_0) + \Delta E_{col}(T_0), \quad (2.6)$$

where $\Delta E_{rad/col}$ is the radiative/collisional energy loss, T_0 is the true initial QGP temperature, and T_0' is the new temperature.

We conclude this section with a discussion of the possible errors due to the neglect of the transverse QGP motion and the use of a flat initial entropy density. We begin with the errors due to the neglect of the QGP transverse flow. It was shown long ago by Baier, Mueller and Schiff [54], within the BDMPS formalism [2], that the flow corrections to predictions obtained using the Bjorken model should be small. This occurs due to an almost complete compensation between the enhancement of parton energy loss caused by increase of the fireball size and its suppression caused by reduction of the transport coefficient due to the QGP expansion. More recently, a detailed numerical analysis of the flow effects in jet quenching at the RHIC and LHC energies, based on the pQCD ansatz for the radiative parton energy loss, performed by Betz and Gyulassy [55] confirmed that the effect of the QGP transverse expansion on the medium suppression of high- p_T spectra is small. In [55] it was found that for 0.2 TeV Au+Au and 2.76 TeV Pb+Pb collisions the change of R_{AA} due to the transverse flow is $\lesssim 1 - 2\%$ (see Fig. 2 of [55]), and it holds both for central and noncentral collisions. The results of [55] show that for heavy ion collisions the errors of our predictions due to the neglect of the QGP transverse expansion should be small. It is important that for noncentral 0.2 TeV Au+Au collisions for 20 – 30% centrality bin the authors of [55] obtained very small flow corrections to R_{AA} both for the jet azimuthal angle $\phi \sim 0$ and $\phi \sim \pi/2$ (i.e., for the jet directions along the short and long fireball semi-diameters). For Au+Au collisions in 20 – 30% centrality bin the short fireball semi-diameter is ~ 2.5 fm. Since this size is close to the oxygen radius, one can conclude that the flow correction to R_{AA} in O+O collisions should be small. For the mQGP produced in pp collisions the fireball radius (see Eq. (3.4) below) is smaller than the short fireball semi-diameter for Au+Au collisions for 20 – 30% centrality by just $\sim 40\%$. Due to the smaller QGP temperature (see Eq. (3.5) below) the QGP sound velocity for pp collisions should be smaller than that for Au+Au collisions. This can reduce somewhat the transverse QGP velocity (which is approximately proportional to the QGP squared sound velocity [56]) for pp collisions. The above facts show that the magnitudes of the QGP transverse flow for 0.2 TeV Au+Au collisions for 20 – 30% centrality bin and pp collisions should not differ drastically. Therefore, there is no reason to expect that the flow correction to R_{pp} can be dramatically larger than that found in [55] for R_{AA} in noncentral Au+Au

collisions. Thus, one can conclude that the errors of our predictions due to the use of the Bjorken model should be quite small.

The situation with the errors due to the use a flat initial entropy distribution in some sense is similar to that for the neglect of the transverse flow. In this case one can also expect a strong compensation between the enhancement of the parton energy loss in the regions where the density is overestimated and its suppression in the regions where the density is underestimated. The jet configurations that can potentially lead to the incomplete compensation are the jet production near the surface of the fireball, when $R_{AA} \sim 1$ for the jets heading outward, and $R_{AA} \ll 1$ for the ones heading to the core of the fireball. This nonlinear effect is possible for heavy ion collisions, but cannot be important for small systems. In general, it is clear that for small systems the sensitivity of jet quenching to the form of the fireball density should be weak, since for such systems we have a situation where the typical formation length for induced gluon emission is of the order of the fireball size or larger. In such a regime the form of the density profile along the fast parton trajectory is not very important, and the parton energy loss is mostly controlled by the total amount of the matter traversed by fast parton. As far as the possible errors in R_{AA} for heavy ion collisions are concerned, even if they are several times larger than the flow corrections found in [55], they can lead only to a relatively small change of the parameters fitted from heavy ion data. For instance, for $R_{AA} \sim 0.2$ a change of R_{AA} by $\sim 20\%$ can be mimicked by changing α_s by $\sim 3\%$ ². Note that the necessary change of α_s to compensate the errors $\sim 20\%$ in R_{AA} for heavy ion collisions will translate to the errors $\lesssim 10\%$ in $R_{AA,pp} - 1$ for small system. Thus, it is clear that the approximation of a flat QGP density cannot spoil significantly the quality of the extrapolation of the jet quenching predictions from heavy ion collisions to collisions of small systems. It is worth noting that, in principle, even for an accurate hydrodynamic fireball evolution it is impossible to avoid the errors of the order of $\sim 10\%$ in $R_{AA,pp} - 1$ in extrapolating the theoretical predictions from heavy ion collisions to small system collisions, because there are also other considerable theoretical uncertainties in jet quenching calculations (e.g. related to the treatment of multiple gluon emission and to the choice of the number density of the color centers, which is the basic input to calculation of the induced gluon spectrum).

3 Models of the QGP fireballs for AA and pp collisions

We perform calculations for simple Bjorken's 1+1D expansion [48] of the QGP. It gives the entropy density $s(\tau)/s(\tau_0) = \tau_0/\tau$, where τ_0 is the thermalization time. At $\tau < \tau_0$ we use a linear parametrization $s(\tau) = s(\tau_0)\tau/\tau_0$. We set $\tau_0 = 0.5$ fm both

²This estimate can be easily obtained from the analytical relation between the energy loss and the medium suppression factor derived in [39], considering that the radiative energy loss is dominated by the $N = 1$ rescattering term (which is $\propto \alpha_s^3$).

for AA and pp collisions. But to understand sensitivity of the results to τ_0 , we also perform calculations for $\tau_0 = 0.8$ fm. As in our previous jet quenching analyses, we model QGP by a system of the static Debye screened color centers [1]. We use the ideal gas model to relate the number density of the QGP constituents to the entropy density. This gives the effective number density of the triplet color centers $n(z) = bT^3(z)$ with $b = 9\xi(3)(N_f + 4)/\pi^2 \approx 7.125$ (for $N_f = 2.5$). As was said above, we use the fireball model with a uniform density distribution in the transverse plane.

3.1 The QGP fireball in AA collisions

Let us start with AA collisions. To fix the average initial QGP entropy density for AA collisions we use the relation [48]

$$s_0 = \frac{C}{\tau_0 S_f} \frac{dN_{ch}(AA)}{d\eta}, \quad (3.1)$$

where S_f is the area of the overlap region of two colliding nuclei, and $C = dS/dy / dN_{ch}(AA)/d\eta \approx 7.67$ [57] is the entropy/multiplicity ratio. We calculate $dN_{ch}(AA)/d\eta$ in the Glauber wounded nucleon model [58] with parameters of the model as in our Monte-Carlo Glauber analyses [59, 60], which describe very well data on the midrapidity $dN_{ch}/d\eta$ in 0.2 TeV Au+Au [61], 2.76 [62] and 5.02 TeV [63] Pb+Pb, and 5.44 TeV Xe+Xe [64] collisions. For heavy nuclei we use the Woods-Saxon nuclear density $\rho_A(r) = \rho_0/[1 + \exp((r - R_A)/d)]$. For Pb nucleus we take the parameters $R_A = 6.62$ and $d = 0.546$ fm, as in the PHOBOS Glauber model [65], and for Xe nucleus we take $d = 0.54$ fm and $R_A = (1.12A^{1/3} - 0.86/A^{1/3})$ fm, as in the GLISSANDO Glauber model [66] (it gives $R_A \approx 5.49$ fm). For our basic version we define S_f for overlap of two circles with radius $R = R_A + kd$ with $k = 2$ (R_A and d are the parameters of the Woods-Saxon nuclear density). To understand the sensitivity of the results to the choice of k , we also performed calculations for $k = 3$. The range $2 \lesssim k \lesssim 3$ seems to be reasonable for determining the fireball size, because, on the one hand, it guarantees that the fraction of the lost QGP volume is small. On the other hand, for such values of k our ansatz with a flat fireball density does not lead to a considerable redistribution of the QGP density into regions where the true QGP density should vanish. Our calculations give a small variation of R_{AA} in heavy ion collisions with k in the range $2 \lesssim k \lesssim 3$ (see below).

For O+O collisions we performed calculations for the harmonic oscillator shell model nuclear density

$$\rho_A(r) = \frac{4}{\pi^{3/2} r_A^3} \left[1 + \frac{A-4}{6} \left(\frac{r}{r_A} \right)^2 \right] \exp(-r^2/r_A^2),$$

$$r_A^2 = \left(\frac{5}{2} - \frac{4}{A} \right)^{-1} (\langle r_{ch}^2 \rangle_A - \langle r_{ch}^2 \rangle_p) \quad (3.2)$$

with $\langle r_{ch}^2 \rangle_A = 7.29 \text{ fm}^2$ for ^{16}O and $\langle r_{ch}^2 \rangle_p = 0.7714 \text{ fm}^2$ [66]. Also, to understand the sensitivity of the results to the ^{16}O nuclear density we have performed calculations for the Woods-Saxon density. For the Woods-Saxon oxygen nuclear density we take $d = 0.513 \text{ fm}$ [67] and $R_A = 2.2 \text{ fm}$ (fixed through the condition of equal $\langle r_{ch}^2 \rangle$ for the Woods-Saxon and the harmonic oscillator shell model nuclear density (3.2)). Our calculations show that the difference between R_{AA} for the harmonic oscillator shell model and for the Woods-Saxon one is very small for the whole range of centrality. We therefore present results only for the oscillator shell model nuclear density. Similarly to heavy ion collisions, for O+O collisions we define S_f for overlap of two circles with radius $R = R_A + kd$ and $k = 2$, where R_A and d the parameters of the Woods-Saxon nuclear density (both for the harmonic oscillator shell model density and the Woods-Saxon one). For heavy ions the results are not very sensitive to variation of the nuclear geometry parameter k . But for light nuclei the variation of R_{AA} with k may be more noticeable, since the ratio of the nuclear surface thickness to the nuclear radius becomes larger. To illustrate dependence of the result on k , for O+O collisions we also present results for $k = 3$.

Fig. 1 shows the centrality dependence of the initial QGP temperature obtained within the Glauber model with the help of the relation (3.1) for heavy ion and O+O collisions. We show the results for the ideal gas model, when $s(T) = aT^3$ with $a = \frac{4\pi^2}{15} (8/3 + 7N_f/4)$ ($a \approx 18.53$, if one takes $N_f = 2.5$). The QGP temperature calculated via (3.1) for the lattice entropy density [47] is somewhat bigger than that for the ideal gas model (by $\sim 5 - 10\%$ at $T \sim 300 - 450$, and by $\sim 15 - 25\%$ at $T \sim 150 - 200 \text{ MeV}$). From Fig. 1 one can see that for 7 TeV O+O collisions the initial fireball temperature is qualitatively similar to that for 0.2 TeV Au+Au collisions. We therefore expect the QGP formation and jet quenching in 7 TeV O+O collisions. However, for 0.2 TeV O+O collisions the initial temperature for centrality $\lesssim 30\%$ is comparable to that expected for pp collisions (see below). For this reason, there is some doubt whether QGP formation in 0.2 TeV O+O collisions is possible, if there is no mQGP formation in pp collisions. But one should bear in mind that O+O collisions have better conditions for collectivity in the final state, because in this case the Knudsen number becomes bigger by a factor of 2 as compared to that for pp collisions. In the present analysis we assume that in 0.2 TeV O+O collisions a QGP is formed.

For a flat entropy distribution the model with the almond shaped fireball with two cups somewhat overestimates the anisotropy coefficient ϵ_2 , as compared to that calculated with an accurate b -dependent entropy density [11]. This fact is immaterial for R_{AA} , which is practically insensitive to azimuthal asymmetry of the fireball. But for calculation of the flow coefficient v_2 this model is too crude. In order to have in our calculations the fireball ellipticity which coincides with that for the accurate Glauber model fireball density, as in [11], we transform the almond shaped region into an elliptic one (of the same area). We perform calculations of v_2 for two choices

of the fireball eccentricity ϵ_2 . For the first variant, we calculate ϵ_2 in the optical Glauber wounded nucleon model, and for the second variant we use ϵ_2 obtained in the Monte-Carlo Glauber model of [59, 60]. The Monte-Carlo version gives ϵ_2 , which, contrary to the optical model one, does not vanish for central collisions (due to density fluctuations). But for noncentral collisions of heavy nuclei predictions of the optical and Monte-Carlo Glauber models for ϵ_2 do not differ significantly. Our treatment of the flow coefficient v_2 for the Monte-Carlo version of ϵ_2 ignores possible decorrelation between the participant plane and the true reaction plane. The effect of this decorrelation should be small for heavy nuclei (see discussion in [11]). However, for light ion collisions, such as O+O in our case, when the density fluctuations become large, our calculations of v_2 become clearly less robust. It worth noting that for light nuclei even the initial anisotropy coefficient ϵ_2 itself cannot be calculated accurately in the Monte-Carlo Glauber model, because the theoretical predictions become sensitive to the size of the entropy sources in the whole range of centrality. For this reason, our results for v_2 in O+O collisions are of illustrative character. But nevertheless they allow to understand the relation between the initial fireball ellipticity ϵ_2 and the flow coefficient v_2 for light nucleus collisions. We perform calculation of v_2 using ϵ_2 for the Gaussian sources with width 0.7 fm. In Fig. 2 we show the theoretical prediction for ϵ_2 for 0.2 and 7 TeV O+O collisions, obtained in the optical Glauber wounded nucleon model and in the Monte-Carlo one, which we use in our calculations of v_2 . To illustrate the sensitivity of ϵ_2 to the source width in the Monte-Carlo scheme we also plot in Fig. 2 predictions for the Gaussian width 0.4 fm. From Fig. 2 one sees that there is a significant difference between the results for the optical and Monte-Carlo versions, and that the Monte-Carlo model ϵ_2 is rather sensitive to the entropy source size. The curves for ϵ_2 for heavy ion collisions can be found in [11].

For AA collisions we use the medium life/freeze-out time $\tau_{f.o.} \approx 1.05 \times (dN_{ch}/d\eta)^{1/3}$, which is supported by the pion interferometry at RHIC [68] and LHC [69]. However, the exact value of the QGP fireball life time is not very crucial to our analysis, since the jet quenching effect of the final stage with $\tau \sim \tau_{f.o.}$ is very small [11, 32]. Note that, from the viewpoint of jet quenching, the nature of the medium in the final stage, whether it is QGP or hadron gas, is not vary crucial, because for a given entropy the energy loss in QGP and hadronic gas turn out to be close to each other [70].

3.2 The mQGP fireball parameters for pp collisions

We now come to the mQGP fireball in pp collisions. Our treatment of the mQGP fireball is similar to that of Ref. [30]. To fix T_0 , we use the relation (3.1) with $dN_{ch}(AA)/d\eta$ replaced by the UE multiplicity density in pp collisions $dN_{ch}^{ue}(pp)/d\eta$. We take $S_f = \pi R_f^2$, where R_f is the effective radius of the mQGP fireball in the pp collision (effective in the sense that it is an average radius for the whole range of the

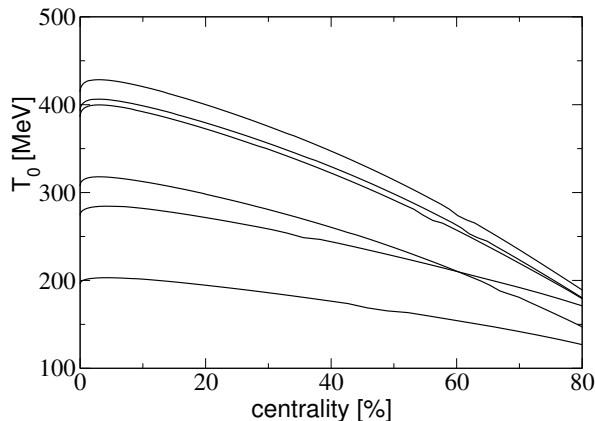


Figure 1. Centrality dependence of the initial fireball temperature at $\tau_0 = 0.5$ fm for the ideal gas model obtained in the Glauber model via the average entropy density for (from top to bottom at low centrality): 5.02 and 2.76 TeV Pb+Pb, 5.44 TeV Xe+Xe, 0.2 TeV Au+Au, 7 and 0.2 TeV O+O collisions.

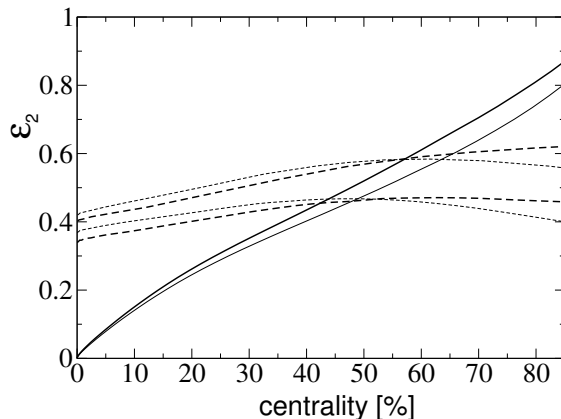


Figure 2. Centrality dependence of the initial fireball eccentricity ϵ_2 for O+O collisions at $\sqrt{s} = 0.2$ TeV (thin lines) and 7 TeV (thick lines) calculated in the optical (solid) and in the Monte-Carlo (dashed) Glauber wounded nucleon model. The curves for the Monte-Carlo version are obtained for the Gaussian width parameter of the entropy sources (top to bottom) 0.4 and 0.7 fm.

impact parameter). We determine R_f via the UE multiplicity density $dN_{ch}/d\eta$ using the prediction for R_f obtained in numerical simulations performed in [71] within the IP-Glasma model [72]. We use the parametrization of R_f from [71] as a function of dN_g/dy given in [73]

$$R_f = 1 \text{ fm} \times f_{pp} \left(\sqrt[3]{dN_g/dy} \right),$$

$$f_{pp}(x) = \begin{cases} 0.387 + 0.0335x + 0.274x^2 - 0.0542x^3 & \text{if } x < 3.4, \\ 1.538 & \text{if } x \geq 3.4. \end{cases} \quad (3.3)$$

We take $dN_g/dy = b dN_{ch}/d\eta$ with $b = C45/2\pi^4\xi(3) \approx 2.13$. For pp collisions at $\sqrt{s} = 0.2$ we calculate the UE multiplicity density using the K_{ue} from PHENIX measurement [21] and the minimum bias non-single-diffractive event multiplicity density $dN_{ch}^{mb}/d\eta = 2.65$ from the UA1 Collaboration [74]. In the plateau region this gives $dN_{ch}^{ue}/d\eta \approx 5.79$. We evaluate the UE multiplicity at $\sqrt{s} = 2.76$ and 5.02 TeV by interpolating the ATLAS data [22] between $\sqrt{s} = 0.9$ and 7 TeV that give in the plateau region $dN_{ch}^{ue}/d\eta \approx 7.5$ and 13.9. Assuming that $dN_{ch}^{ue}/d\eta \propto s^\delta$, we obtained $dN_{ch}^{ue}/d\eta \approx 10.5(12.6)$ for $\sqrt{s} = 2.76(5.02)$ TeV. Using these values of $dN_{ch}^{ue}/d\eta$ we obtain

$$R_f[\sqrt{s} = 0.2, 2.76, 5.02, 7 \text{ TeV}] \approx [1.26, 1.44, 1.49, 1.51] \text{ fm}. \quad (3.4)$$

Then, using the above values of $dN_{ch}^{ue}/d\eta$ and R_f from (3.4), we obtain for the initial temperature of the mQGP fireball for the ideal gas entropy and for the lattice entropy [47] (numbers in brackets)

$$T_0[\sqrt{s} = 0.2, 2.76, 5.02, 7 \text{ TeV}] \approx [195(226), 217(247), 226(256), 232(261)] \text{ MeV}. \quad (3.5)$$

As one can see, for the lattice entropy T_0 is larger by $\sim 10 - 15\%$ than T_0 determined in the ideal gas model.

4 Numerical results

4.1 Optimal κ from the χ^2 fit

We have adjusted the free parameter κ by χ^2 fitting of the LHC data on R_{AA} for heavy ions collisions for centrality $\lesssim 30\%$ and the transverse momentum $10 < p_T < 120$ GeV. We have used data from ALICE [75], ATLAS [76], and CMS [77] for 2.76 TeV Pb+Pb collisions; from ALICE [78], ATLAS [79], and CMS [80] for 5.02 TeV Pb+Pb collisions; and for 5.44 TeV Xe+Xe collisions from ALICE [81], ATLAS [82], and CMS [83]. As usual, we define χ^2 as

$$\chi^2 = \sum_i^N \frac{(f_i^{exp} - f_i^{th})^2}{\sigma_i^2}, \quad (4.1)$$

where N is the number of the data points, and $\sigma_i^2 = \sigma_{i,stat}^2 + \sigma_{i,sys}^2$. We calculate χ^2 using the theoretical R_{AA} obtained with the help of a cubic spline interpolation in κ using a pre-prepared grid with steps $\Delta\kappa/\kappa \sim 0.1$. The optimal values of κ , and the corresponding $\chi^2/d.p.$ (χ^2 per data point), for the versions with and without mQGP formation in pp collisions, obtained using the geometrical parameter $k = 2$ and the parametrization (2.5) with $c = 0.8$, are summarized in Table I. In Table I we present

	Without mQGP			With mQGP		
	κ	95% CI	$\chi^2/d.p.$	κ	95% CI	$\chi^2/d.p.$
Pb+Pb 2.76 TeV	$3.44^{+0.04}_{-0.04}$	(3.16, 3.7)	0.75	$2.57^{+0.05}_{-0.05}$	(2.3, 2.82)	1
Pb+Pb 5.02 TeV	$3.47^{+0.06}_{-0.06}$	(3.02, 3.82)	0.76	$2.5^{+0.08}_{-0.08}$	(2.1, 2.8)	1
Xe+Xe 5.44 TeV	$3.59^{+0.08}_{-0.08}$	(2.92, 4.19)	0.47	$2.52^{+0.109}_{-0.12}$	(2, 3.3)	0.51
All LHC data	$3.47^{+0.03}_{-0.03}$	(3.13, 0.3.78)	0.68	$2.55^{+0.04}_{-0.04}$	(2.16, 2.88)	0.87

Table 1. Optimal values of κ with 1σ standard errors, 95% CI and corresponding $\chi^2/d.p.$, obtained for $k = 2$, $c = 0.8$ at $\tau_0 = 0.5$ fm, $\tau_{max} = 1.05 \times (dN_{ch}/d\eta)^{1/3}$ for $10 < p_T < 120$ GeV for different energies/processes separately and for all LHC data for scenarios without (left) and with (right) mQGP formation in pp collisions.

results for each energy (and process) separately and for the combined fit for all LHC data. We show for κ the standard errors (i.e. corresponding to $\Delta\chi^2 = 1$), and the 95% confidence intervals (CIs) for the 95% quantile of the χ^2 -distribution. From Table I it is seen that for all the cases we have a quite good fit quality ($\chi^2/d.p. \lesssim 1$). The optimal values of κ for different energies/processes are very similar. We find, as one could expect, that scenario with mQGP formation requires somewhat smaller values of κ (the reduction of κ for this version is ~ 1). We have also performed fitting for the geometrical parameter $k = 3$. In this case, for the optimal κ for all the LHC data we obtained $\kappa \approx 3.74(2.98)$ for scenarios without(with) mQGP formation with a quite good fit quality ($\chi^2/d.p. \sim 0.7$). Our fit for $\tau_0 = 0.8$ fm gives the values of κ that are smaller by $\sim 0.22(0.12)$ for scenarios without(with) mQGP formation. For calculations with $c = 0$ in (2.5), the optimal values of κ are larger than that for $c = 0.8$ by $\sim 0.4(0.05)$ for versions without(with) mQGP formation.

4.2 Predictions for R_{pp} , R_{AA} and azimuthal asymmetry v_2

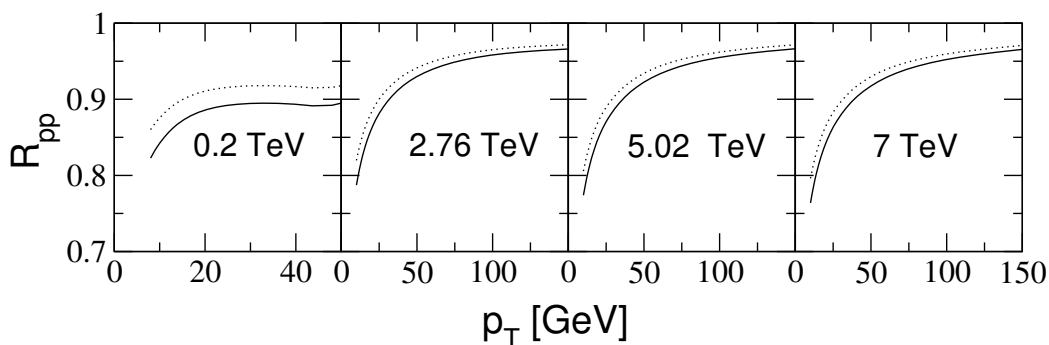


Figure 3. R_{pp} of charged hadrons for 0.2, 2.76, 5.02 and 7 TeV pp collisions from our calculations for $\tau_0 = 0.5$ (solid) and 0.8 fm (dotted) with $\kappa = 2.55$ obtained by fitting all the LHC data on R_{AA} for heavy ion collisions with the geometrical parameter $k = 2$.

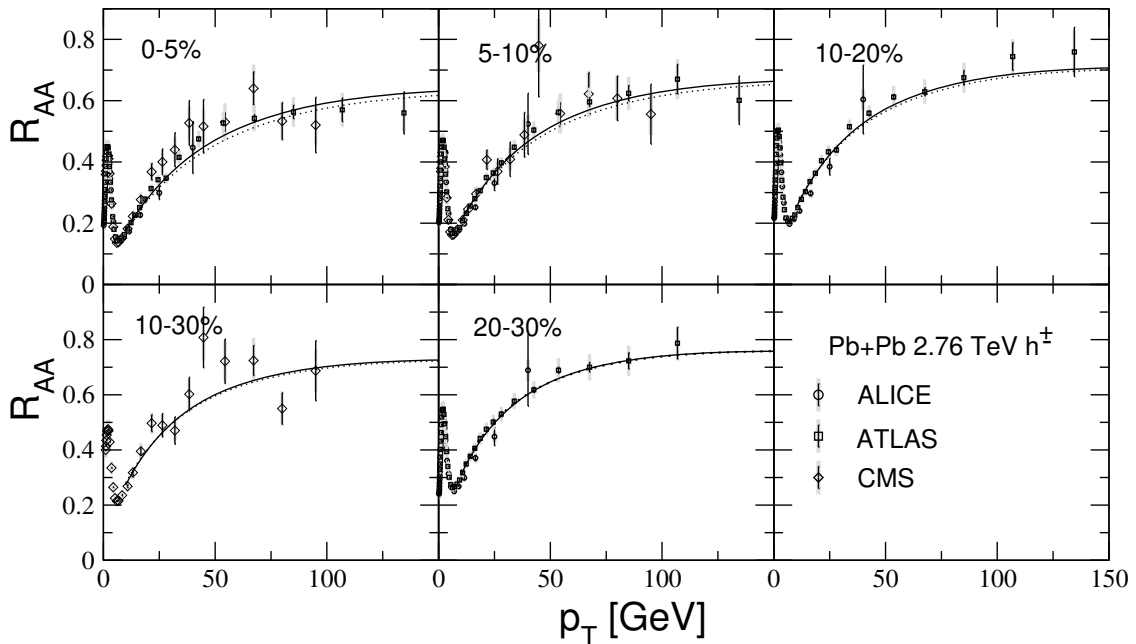


Figure 4. R_{AA} of charged hadrons for 2.76 TeV Pb+Pb collisions from our calculations with $k = 2$, $c = 0.8$, $\tau_0 = 0.5$ fm for scenarios without (solid) and with (dotted) mQGP formation in pp collisions for the optimal parameters $\kappa = 3.44$ and 2.57 obtained by fitting R_{AA} in the range $10 < p_T < 120$ GeV. Data points are from ALICE [75], ATLAS [76], and CMS [77].

The results for R_{pp} , obtained for the optimal value $\kappa = 2.55$ for $c = 0.8$, are shown in Fig. 3 for the RHIC energy $\sqrt{s} = 0.2$, and the LHC energies $\sqrt{s} = 2.76$, 5.02 , and 7 TeV. To illustrate sensitivity of the results to the value of τ_0 , we show in Fig. 3 the results for $\tau_0 = 0.8$ fm. As one can see, the difference between the results for $\tau_0 = 0.5$ and 0.8 fm is rather small, especially for the LHC energies. The curves for $\tau_0 = 0.8$ fm in Fig. 3 are obtained with the optimal κ for R_{AA} for $\tau_0 = 0.5$ fm. The results for R_{pp} obtained for the value of κ adjusted from fit of R_{AA} with $\tau_0 = 0.8$ fm are very close to that shown in Fig. 3 for $\tau_0 = 0.5$ fm. The curves shown in Fig. 3 correspond to our fit of the heavy ion data with the geometrical parameter $k = 2$. Calculations of R_{pp} with $\kappa \approx 2.98$ obtained from the heavy ion fit with $k = 3$ give a small ($\lesssim 5\%$) decrease of $1 - R_{pp}$. Thus, our results for R_{pp} are quite stable against variation of the parameter k used for calculations of R_{AA} in heavy ion collisions. Note that the specific form (3.3) of the fireball radius R_f from the IP-Glasma model, used in our calculations, is practically unimportant for R_{pp} , because, at a given UE multiplicity density, it varies very slowly with R_f . We observed that at $p_T \sim 10 - 20$ GeV the variation of R_{pp} with the fireball radius for the interval $R_f/1.3 - R_f 1.3$ (with R_f given by (3.4)) is $\lesssim 2\%$, and at $p_T \gtrsim 50$ GeV it becomes $\lesssim 0.3\%$. Note that the R_{pp} obtained in the present work is closer to 1

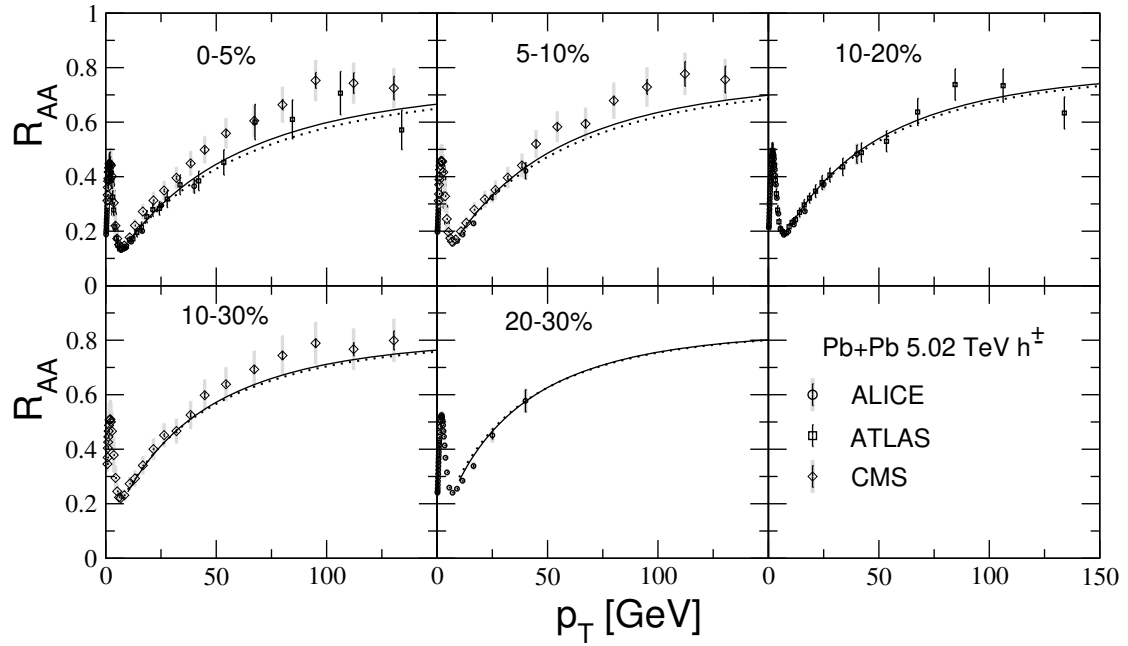


Figure 5. Same as in Fig. 4 for $\sqrt{s} = 5.02$ TeV for the optimal parameters $\kappa = 3.47$ and 2.5. Data points are from ALICE [78], ATLAS [79], and CMS [80].

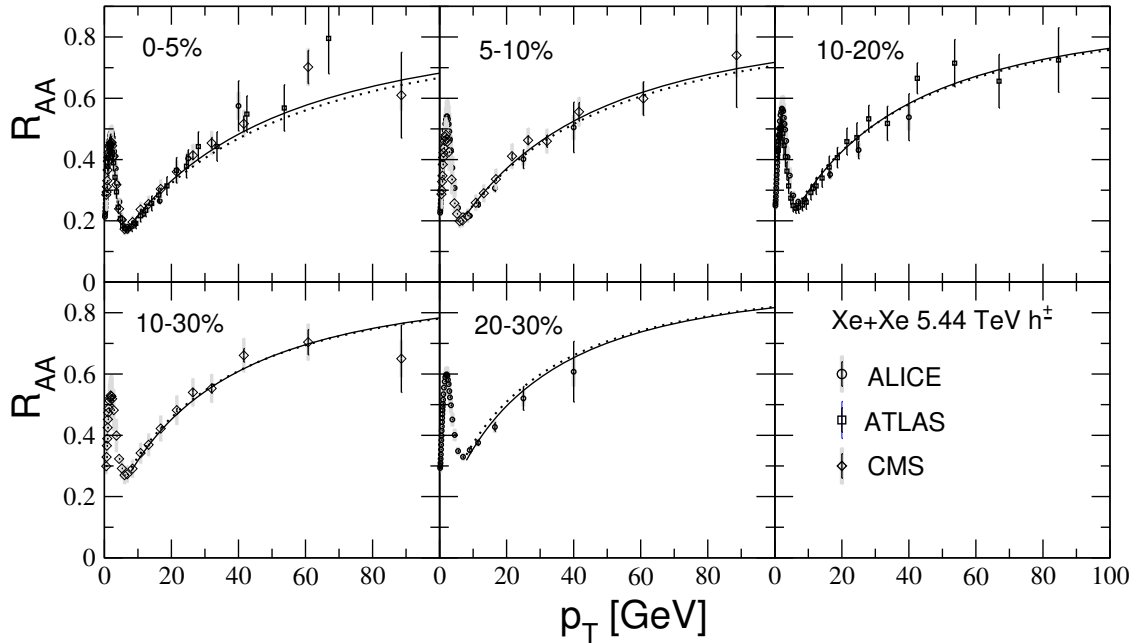


Figure 6. Same as in Fig. 4 for 5.44 TeV Xe+Xe collisions for the optimal parameters $\kappa = 3.59$ and 2.52. Data points are from ALICE [81], ATLAS [82], and CMS [83].

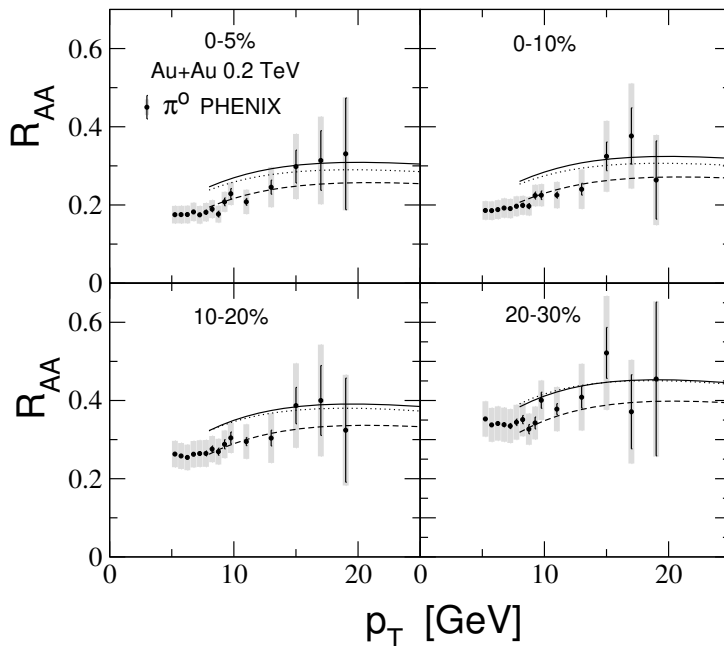


Figure 7. Same as in Fig. 4 for R_{AA} of π^0 in 0.2 TeV Au+Au collisions for the optimal parameters $\kappa = 3.47$ and 2.55 determined by fitting all the LHC data on R_{AA} in Pb+Pb and Xe+Xe collisions. The dashed curves show the results for $\kappa = 2.55$, corresponding to the mixed scenario with mQGP formation in pp collisions only at the LHC energies. Data points are from PHENIX [84].

than the band for R_{pp} given in our previous analysis [30]. These calculations were performed for a temperature independent α_s^{fr} , invariable in the whole QGP fireball. This entails some arbitrariness in the predictions for R_{pp} as different choices of α_s^{fr} for large and small size QGPs are possible.

In Figs. 4–6 we compare our results for R_{AA} for charged hadrons with the LHC data for 2.76 and 5.02 TeV Pb+Pb and 5.44 TeV Xe+Xe collisions used in our χ^2 fitting. We show the curves for the optimal values of κ for the scenarios with and without mQGP formation. In Figs. 4–6 we show the results for the geometrical parameter $k = 2$. For a given κ obtained with $k = 2$, R_{AA} at $k = 3$ decreases by $\sim 5 - 10\%$ at $p_T \sim 10 - 20$ GeV and by $\sim 1 - 3\%$ at $p_T \sim 50 - 100$ GeV as compared to R_{AA} for $k = 2$. The difference between R_{AA} for $k = 2$ and $k = 3$ for the optimal values of κ is very small (typically $\lesssim 1 - 2\%$) at all p_T . Therefore we do not show the curves for $k = 3$. From Figs. 4–6 one can see that for optimal values of κ the difference between theoretical R_{AA} for our two scenarios is very small. From Figs. 4–6 one can see that the theoretical curves for the scenarios with and without mQGP formation in pp collisions agree quite well with experimental data. Our results for R_{AA} obtained for $\tau_0 = 0.8$ fm (not shown) turn out to be very close to that for $\tau_0 = 0.5$ fm. Even if R_{AA} for $\tau_0 = 0.8$ fm is calculated with the optimal value of κ

obtained for $\tau_0 = 0.5$ fm, it grows just by $\sim 1 - 2\%$. This says that jet quenching in heavy ion collisions is not very sensitive to the initial stage of the fireball evolution. The results of our calculations for $c = 0$ in the parametrization (2.5) are very close to that for $c = 0.8$ (shown in Figs. 4–6), therefore we do not plot them as well.

In Fig. 7 we compare the results for R_{AA} of π^0 -mesons in 0.2 TeV Au+Au collisions with the data from PHENIX [84]. The theoretical curves are obtained with the optimal values of κ adjusted by fitting the LHC data. Note that a joint fit of the RHIC and the LHC data practically does not change the optimal values of κ obtained from the LHC data, because the number of the data points for the LHC data set is much bigger than for the PHENIX data. From Fig. 7 one can see that the theoretical curves somewhat overshoot the data at $p_T \sim 10$ GeV. However, the discrepancy between the results for RHIC and the LHC for the T -dependent α_s is much smaller than in the case of calculations with a unique, temperature independent, α_s [11]. Since conditions for formation of a mQGP in pp collisions are less favorable than for the LHC energies, it is interesting to compare the RHIC data on R_{AA} also for an intermediate scenario when mQGP formation in pp collisions occurs only at the LHC energies. In this case the theoretical R_{AA} for 0.2 TeV Au+Au collisions should be calculated without $1/R_{pp}$ factor for the optimal κ fixed in the scenario with mQGP formation from the LHC data on R_{AA} . In Fig. 7 we show the results for this case, using $\kappa = 2.55$ obtained in the scenario with mQGP formation at the LHC energies. As one can see, it gives somewhat better agreement with the PHENIX data [84]. This fact supports the intermediate scenario without a fully developed hydrodynamic evolution of the QCD matter in 0.2 TeV pp collisions. Of course, this interpretation of the discrepancy between α_s for the RHIC and the LHC energies is quite speculative, because our calculations include several simplifications, and the errors for the PHENIX data on R_{AA} at $p_T \gtrsim 10$ GeV are rather large.

In Figs. 8 and 9 we compare the theoretical predictions for the flow coefficient v_2 with available experimental data for 2.76 [85–87] and 5.02 [88, 89] TeV Pb+Pb collisions. We show the theoretical results for the fireball azimuthal asymmetry ϵ_2 obtained in the optical Glauber model and for the Monte-Carlo one (for the Gaussian entropy sources with width $\sigma = 0.7$ fm). The most significant difference in predictions of the optical and the Monte-Carlo versions is for the most central (0-5%) collisions. Although v_2 was not included into our χ^2 analysis, the results for v_2 are in qualitative agreement with what is seen in the LHC data. Of course, one should bear in mind, that results for the azimuthal dependence are less robust. For instance, for v_2 , which is sensitive to a delicate balance between jet modification in the directions along the short and long fireball semi-diameters, the errors due to the neglect of the transverse QGP motion and due to the use of a flat initial entropy distribution can potentially be larger than for the azimuthally averaged R_{AA} . Note that for v_2 the difference in the theoretical predictions for scenarios with and without mQGP is more pronounced than for R_{AA} . It is due to some enhancement of the strength of jet quenching for

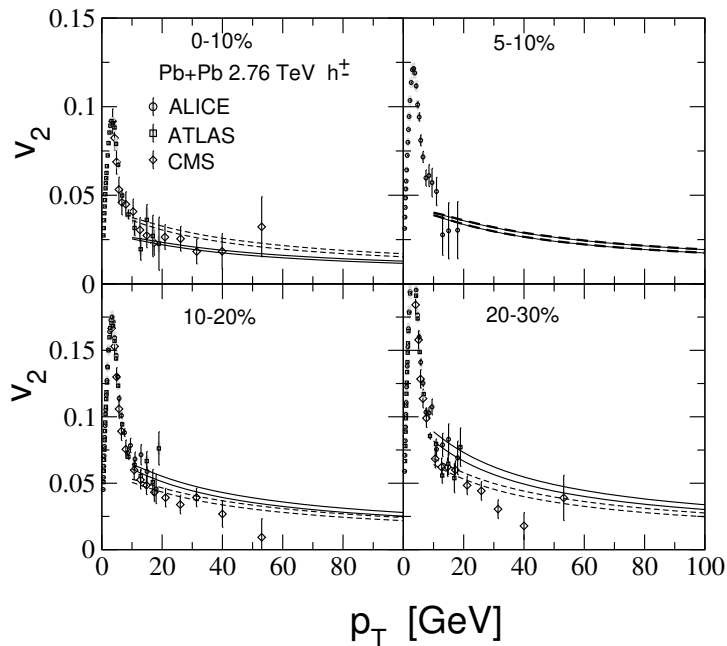


Figure 8. v_2 of charged hadrons in 2.76 TeV Pb+Pb collisions for the initial fireball eccentricity ϵ_2 calculated in the optical (solid) and Monte-Carlo (dashed) Glauber model for scenarios without and with (bottom to top) mQGP formation in pp collisions. The parameters are the same as for Fig. 4. Data points are from ALICE [85], ATLAS [86], and CMS [87].

the scenario with mQGP formation (due to smaller value of κ) as compared to the one without mQGP. Contrary to the case of R_{AA} , for v_2 this difference is now not compensated by the presence of the $1/R_{pp}$ factor, because this factor is immaterial for calculation of the azimuthal asymmetry.

Thus, we have established that the scenarios with and without mQGP can describe equally reasonably jet quenching in heavy ion collisions. Now, using the optimal values of κ , adjusted to fit R_{AA} for heavy ion collisions, we can calculate R_{AA} for O+O collisions. In Figs. 10 and 11 we show the results for R_{AA} in 0.2 and 7 TeV O+O collisions for scenarios with and without mQGP formation in pp collisions. We present results for three narrow centrality bins and for the minimum bias R_{AA} (i.e., for 0 – 100% centrality interval). The latter quantity is particularly convenient for comparison with experiment, because for light ion collisions, due to large multiplicity fluctuations, the impact parameter becomes less correlated with centrality, which is defined experimentally via charged multiplicity. For $\sqrt{s} = 0.2$ TeV, as in Fig. 7 for 0.2 TeV Au+Au collisions, we also show predictions for the intermediate scenario with mQGP formation in pp collisions only at the LHC energies. As one can see, this scenario leads to the smallest R_{AA} for 0.2 TeV O+O collisions. To illustrate sensitivity of the results to τ_0 , in Figs. 10 and 11 we present the results for $\tau_0 = 0.5$

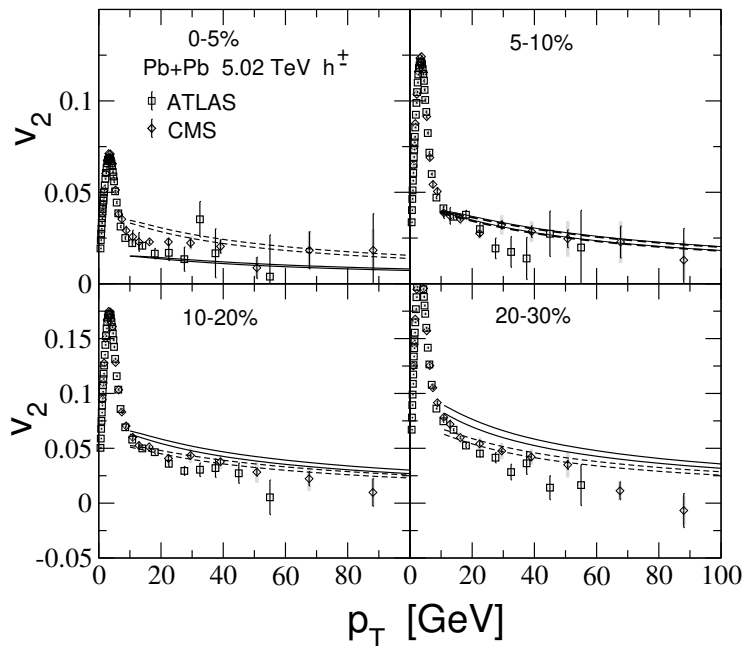


Figure 9. Same as in Fig. 8 for $\sqrt{s} = 5.02$ TeV. The parameters are the same as for Fig. 5. Data points are from ATLAS [88] and CMS [89].

and 0.8 fm. As one can see, the difference between predictions for these two values of τ_0 is rather small, especially for $\sqrt{s} = 7$ TeV. In Figs. 10 and 11, in addition to the real R_{AA} , we also plot the modification factor for hadron spectra only due to nuclear modification of the parton distribution functions for AA collisions (which we denote R_{AA}^{pdf}). For light ion collisions, when $R_{AA} \sim 1$, it is reasonable to characterize magnitude of jet quenching by $\Delta R_{AA} = R_{AA}^{pdf} - R_{AA}$. From Figs. 10 and 11 we observe that, both for $\sqrt{s} = 0.2$ and 7 TeV, there is a substantial difference in ΔR_{AA} for scenarios with and without mQGP formation in pp collisions. Thus, although the discrepancy between R_{AA} for these two scenarios are very small for heavy ion collisions, they give very different ΔR_{AA} for light ion collisions. To illustrate dependence of the theoretical predictions on the choice of the nuclear geometry parameter k , which we use to define the overlap region of the colliding nuclei, in Figs. 10 and 11, in addition to the version with $k = 2$, we also plot the results for $k = 3$. As one can see, there is no a significant difference between calculations for $k = 2$ and 3. From Figs. 10 and 11 we can conclude that possible variation of R_{AA} in O+O collisions under change of the parameters k and τ_0 turns out to be smaller than the difference between predictions for our two scenarios without and with mQGP formation in pp collisions.

From Fig. 11 one can see that for 7 TeV O+O collisions the minimum bias ΔR_{AA} for scenarios without and with mQGP formation may differ by a factor of $\sim 1.5 - 2$ at $p_T \sim 50 - 150$ GeV. Nevertheless, the p_T -dependence of R_{AA} for both models are similar. Also, one should bear in mind that R_{AA}^{pdf} has its own theoretical uncertainties.

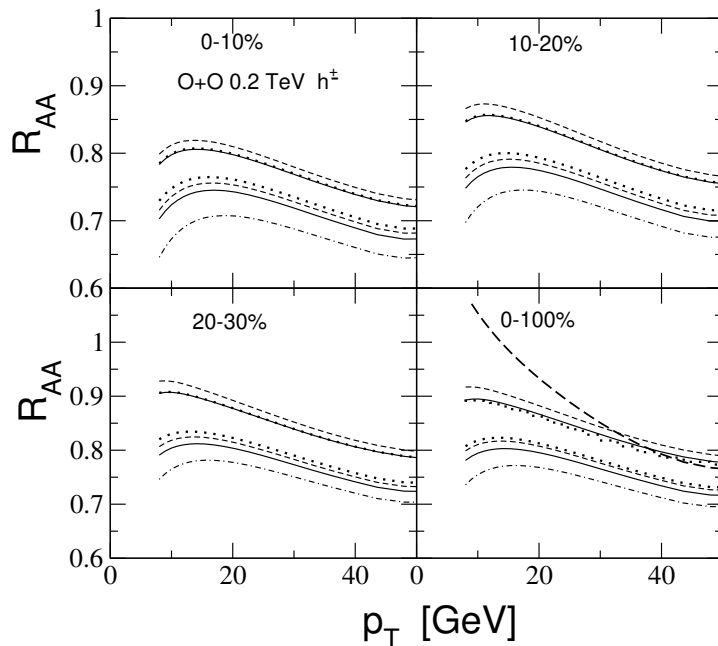


Figure 10. R_{AA} of charged hadrons for 0.2 TeV O+O collisions from our calculations for scenarios (top to bottom) with ($\kappa = 2.55$) and without ($\kappa = 3.47$) mQGP formation in pp collisions. The solid and dashed curves are for $\tau_0 = 0.5$, and the dotted ones are for 0.8 fm. The solid and dotted curves are obtained for the geometrical parameter $k = 2$, and the dashed curves are for $k = 3$ (see text for explanation). The dash-dotted lines show the results (for $k = 2$, $\tau_0 = 0.5$ fm, $\kappa = 2.55$) for the intermediate scenario when mQGP formation in pp collisions occurs at the LHC energies, but it is absent at RHIC. The long dashed line shows R_{AA}^{pdf} .

All this can make it difficult to discriminate between the scenarios without and with mQGP formation from comparison with the future LHC data. From Fig. 10 we observe that for 0.2 TeV O+O collisions the difference between scenarios with and without mQGP formation is somewhat more pronounced than at $\sqrt{s} = 7$ TeV. It is interesting that in this case the minimum bias R_{AA} for the mQGP scenario becomes larger R_{AA}^{pdf} at $p_T \gtrsim 35$ GeV. An observation of such a crossover would support mQGP formation in pp collisions.

In Figs. 12 and 13 we plot the results for the flow coefficient v_2 for the initial fireball azimuthal asymmetry ϵ_2 obtained within the optical Glauber wounded nucleon model and within its Monte-Carlo counterpart. Similarly to v_2 for Pb+Pb collisions, shown in Figs. 8 and 9, we obtain somewhat larger v_2 for scenario with mQGP formation. As already said above, our results for v_2 in O+O collisions are of illustrative character, because for O+O collisions the effect of fluctuations of the initial entropy density is very important. For this reason our purpose is just to demonstrate the relation between the initial fireball ellipticity ϵ_2 and v_2 . From Fig. 13 we observe

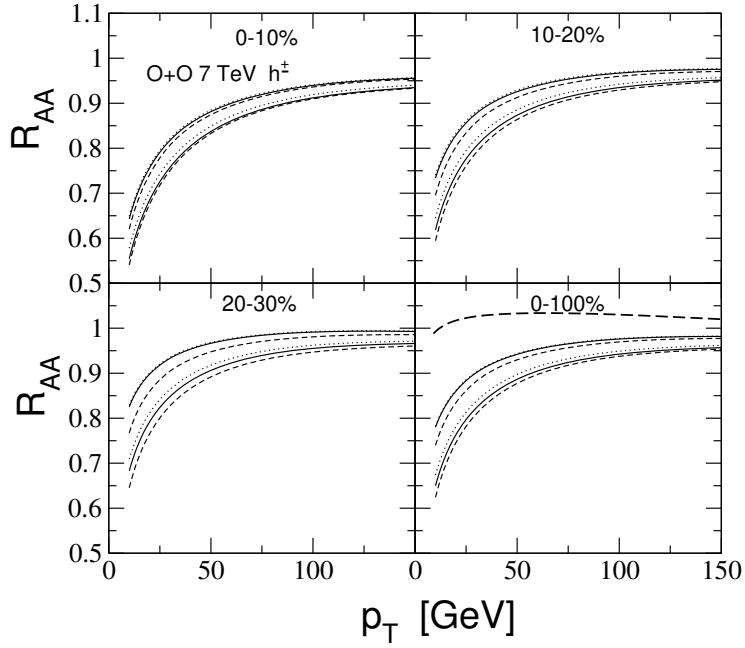


Figure 11. Same as in Fig. 10 (but now without dash-dotted lines) for 7 TeV O+O collisions.

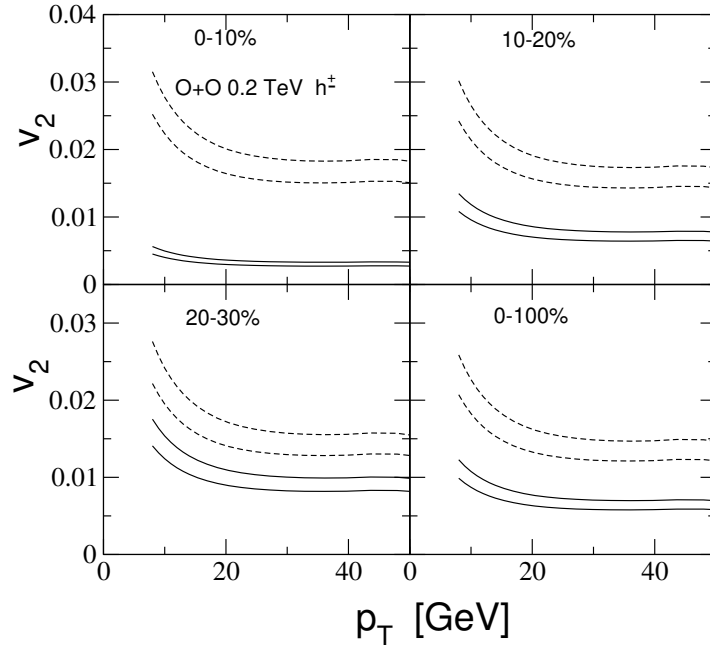


Figure 12. v_2 of charged hadrons in 0.2 TeV O+O collisions for $\tau_0 = 0.5$ for the initial fireball eccentricity ϵ_2 calculated in the optical (solid) and Monte-Carlo (dashed) Glauber model for scenarios without and with (bottom to top) mQGP formation in pp collisions.

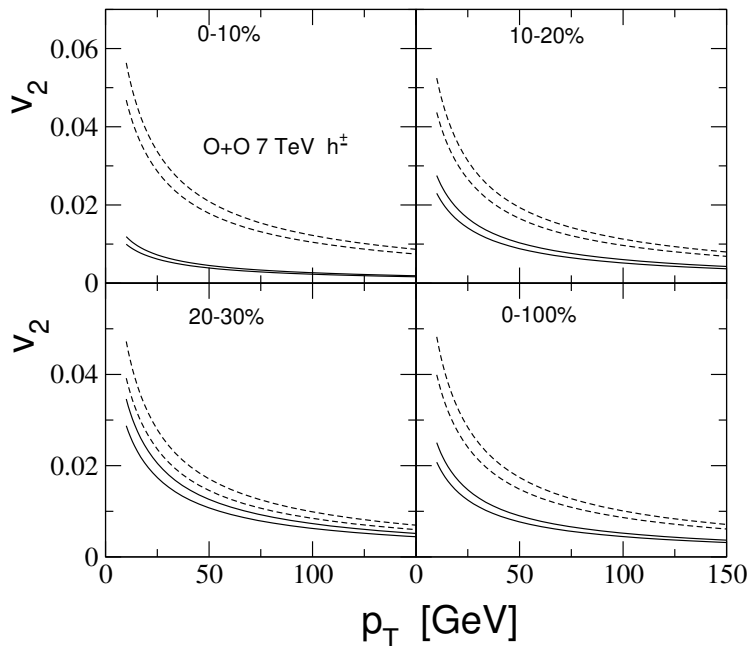


Figure 13. Same as in Fig. 12 for $\sqrt{s} = 7$ TeV.

that for 7 TeV O+O collisions $\epsilon_2/v_2 \sim 20 - 25$ at $p_T \sim 50$ GeV.

4.3 Jet quenching in pA collisions

We have not touched yet jet quenching in pA collisions. Similarly to formula (1.3), the theoretical observable nuclear modification factor for pA collisions is given by $R_{pA} = R_{pA}^{st}/R_{pp}$. Unfortunately, a conclusive comparison with experiment is presently impossible, because the available data on R_{pA} are somewhat contradictory. ALICE measurement [90] gives the minimum bias R_{pA} of charged hadrons in 5.02 TeV p +Pb collisions which is $\sim 0.92 - 1$ at $p_T \gtrsim 10$. More recent ALICE measurement [91] of R_{pA} for π^0 mesons in 8.16 TeV p +Pb collisions also gives R_{pA} which is close to unity at $p_T \gtrsim 10$ GeV. In contrast, the CMS collaboration [92] obtained for charged hadrons in 5.02 TeV p +Pb collisions $R_{pA} \sim 1.1 - 1.19$ at $p_T \gtrsim 10$ GeV. The LHC data from ALICE and CMS seem to exclude the scenario when mQGP formation and jet quenching are absent in pp collisions (i.e., $R_{pp} \approx 1$), but are present in pA collisions (i.e., $R_{pA} < 1$). If one assumes that the data from ALICE [90, 91] are correct, the question arises whether the scenario with mQGP formation, both in pp and pA collisions, can be consistent with R_{pA} measured by ALICE. It is possible if the theoretical nuclear modification factor R_{pA}^{st} is just a little smaller than R_{pp} . Calculations of R_{pA}^{st} require detailed information on the QGP fireball in pA collisions. We have performed preliminary calculations of R_{pA} for 5.02 and 8.16 TeV p +Pb collisions using the fireball parameters obtained by modeling the UE fireball within the Monte-Carlo Glauber wounded nucleon model. The important difference between

the minimum bias events and the jet events in the wounded nucleon Glauber picture is that in the jet events always there is one wounded pN pair participating in the hard parton production, which produces the UE multiplicity density $dN_{ch}^{ue}(pp)/d\eta$ enhanced by the $K_{ue} \sim 2.5$ factor, as compared to the minimum bias multiplicity density $dN_{ch}^{mb}(pp)/d\eta$. This leads to a two component structure of the fireball, with a high density core and the low density peripheral part (related to spectator wounded nucleons, that do not participate in the hard process). Our Monte-Carlo simulation shows that for p +Pb collisions the peripheral fireball part can give $\sim 20 - 30\%$ of the total UE multiplicity density $dN_{ch}^{ue}(pA)/d\eta$. Since the entropy density in the peripheral part is rather small (the ideal gas temperature $\sim 150 - 170$ MeV), one can expect that it should be close to the free-streaming regime, and its effect on jet quenching should be small. The core region of the UE fireball in 5.02(8.16) TeV p +Pb collisions, which can have collective behavior, generates the charged multiplicity density $\sim 23 \pm 3(27 \pm 3)$. Calculations with such charged multiplicity densities give $R_{pA} = R_{pA}^{st}/R_{pp}$ which agrees quite well with the ALICE data [90, 91]. Of course, this analysis is of preliminary character. It is highly desirable to investigate the jet quenching effect of the peripheral part of the fireball (that can be close to the free-streaming regime) and to perform calculations for a realistic fireball density profile accounting for the transverse flow (although we expect that the effect of the density variation and the flow corrections should be small (see section 2)). We leave this, more complicated, calculations for future work.

5 Conclusions

In the present work, we have studied jet quenching for heavy and light ion collisions within the LCPI approach [3] to induced gluon emission. Calculations of the induced gluon spectrum are performed with accurate treatment of the Coulomb effects, using the method suggested in [33]. We account for multiple gluon emission in the approximation of independent gluon radiation [39] in the form suggested in [32] (with some modifications made in [11]). We perform calculations for the temperature dependent running QCD coupling. We use parametrization of $\alpha_s(Q, T)$ which has a plateau around $Q = Q_{fr} \sim \kappa T$ (it is motivated by the lattice calculation of the effective QCD coupling in the QGP [41] and calculations within the functional renormalization group [42]).

We have investigated scenarios with and without mQGP formation in pp collisions, and an intermediate scenario with mQGP formation only at the LHC energies. The parameter κ has been fitted to the LHC data on the nuclear modification factor R_{AA} in 2.76 and 5.02 TeV Pb+Pb, and 5.44 TeV Xe+Xe collisions. We find that predictions of the models with and without mQGP formation in pp collisions are very similar, and both of them lead to quite good description of the LHC heavy ion data on R_{AA} . The theoretical predictions for the flow coefficient v_2 are also in reasonable

agreement with the LHC data. The optimal values of κ , fitted to the LHC data on R_{AA} , lead to reasonable description of the PHENIX data [84] on R_{AA} in 0.2 TeV Au+Au collisions in scenarios with and without mQGP formation in pp collisions. Agreement with the PHENIX data becomes somewhat better for the intermediate scenario with mQGP formation in pp collisions only at the LHC energies. Overall, our analysis shows that the experimental data on jet quenching in heavy ion collisions can equally well be described in scenarios without and with mQGP formation in pp collisions.

Using the optimal values of the parameter κ , obtained by fitting R_{AA} in heavy collisions, we perform calculations of R_{AA} and v_2 for 0.2 and 7 TeV O+O collisions which may be studied in future experiments at RHIC [15] and at the LHC [16–18]. We find that predictions of scenarios with and without mQGP formation for $R_{AA} - R_{AA}^{pdf}$ begin to differ substantially for O+O collisions. However, due to theoretical uncertainties for R_{AA}^{pdf} , and the fact that the p_T -dependence of R_{AA} for both scenarios are similar, it may be difficult to discriminate between the scenarios without and with mQGP formation from comparison with the future LHC data. We find that for 0.2 TeV O+O collisions the difference between scenarios with and without mQGP formation in pp collisions is somewhat more pronounced. Our calculations show that in this case the minimum bias R_{AA} for the mQGP scenario becomes larger R_{AA}^{pdf} at $p_T \gtrsim 35$ GeV.

For the medium modification factor R_{pp} (that is not directly observable quantity) we obtain at $p_T = 10$ GeV $R_{pp} \sim 0.84 - 0.88$ at $\sqrt{s} = 0.2$ TeV, and $R_{pp} \sim 0.77 - 0.82$ at the LHC energies.

Acknowledgments

I am grateful to S. Tripathy for useful communication on some aspects of the recent ALICE results on jet quenching in small collision systems [31]. This work was performed under the Russian Science Foundation grant 20-12-00200 at Steklov Mathematical Institute.

References

- [1] M. Gyulassy and X.N. Wang, Nucl. Phys. B**420**, 583 (1994) [nucl-th/9306003].
- [2] R. Baier, Y.L. Dokshitzer, A.H. Mueller, S. Peigné, and D. Schiff, Nucl. Phys. B**483**, 291 (1997) [hep-ph/9607355].
- [3] B.G. Zakharov, JETP Lett. **63**, 952 (1996) [hep-ph/9607440].
- [4] U.A. Wiedemann, Nucl. Phys. A**690**, 731 (2001) [hep-ph/0008241].
- [5] M. Gyulassy, P. Lévai, and I. Vitev, Nucl. Phys. B**594**, 371 (2001) [hep-ph/0006010].
- [6] P. Arnold, G.D. Moore, and L.G. Yaffe, JHEP **0206**, 030 (2002) [hep-ph/0204343].

- [7] S. Shi, J. Liao, M. Gyulassy, *Chin. Phys.* **C43**, 044101 (2019) [arXiv:1808.05461].
- [8] D. Zigic, I. Salom, J. Auvinen, Marko Djordjevic, and Magdalena Djordjevic, *Phys. Lett.* **B791**, 236 (2019) [arXiv:1805.04786].
- [9] C. Andres, N. Armesto, H. Niemi, R. Paatelainen, and C.A. Salgado, *Phys. Lett.* **B803**, 135318 (2020) [arXiv:1902.03231].
- [10] A. Huss, A. Kurkela, A. Mazeliauskas, R. Paatelainen, W. van der Schee, and U.A. Wiedemann, arXiv:2007.13758.
- [11] B.G. Zakharov, *J. Phys.* **G48**, 055009 (2021) [arXiv:2007.09772].
- [12] V. Khachatryan *et al.* [CMS Collaboration], *JHEP* **1009**, 091 (2010) [arXiv:1009.4122].
- [13] G. Aad *et al.* [ATLAS Collaboration], *Phys. Rev. Lett.* **116**, 172301 (2016) [arXiv:1509.04776].
- [14] K. Dusling and R. Venugopalan, *Phys. Rev.* **D87**, 094034 (2013) [arXiv:1302.7018].
- [15] W. Li, Workshop “Opportunities of OO and pO collisions at the LHC”, 4–10 February 2021, CERN, URL <https://cds.cern.ch/record/2752019>.
- [16] Z. Citronet *al.*, Report on the Physics at the HL-LHC, and Perspectives for the HE-LHC, edited by A. Dainese, M. Mangano, A.B. Meyer, A. Nisati, G. Salam, and M.A. Vesterinen (2019), arXiv:1812.06772.
- [17] R. Bruce, Workshop “Opportunities of OO and pO collisions at the LHC”, 4–10 February 2021, CERN, URL <https://cds.cern.ch/record/2751162>.
- [18] J. Brewer, A. Mazeliauskas, and W. van der Schee, arXiv:2103.01939.
- [19] R. Field, *Acta Phys. Polon.* **B42**, 2631 (2011) [arXiv:1110.5530].
- [20] A.A. Affolder *et al.* [CDF Collaboration], *Phys. Rev.* **D65**, 092002 (2002).
- [21] J. Jia, for the PHENIX Collaboration, contribution to the Quark Matter 2009 Conf., March 30 - April 4, Knoxville, Tennessee; arXiv:0906.3776.
- [22] G. Aad *et al.* [ATLAS Collaboration], *Phys. Rev.* **D83**, 112001 (2011) [arXiv:1012.0791].
- [23] S. Chatrchyan *et al.* [CMS Collaboration], *JHEP* **1109**, 109 (2011) [arXiv:1107.0330].
- [24] B. Abelev *et al.* [ALICE Collaboration], *JHEP* **1207**, 116 (2012) [arXiv:1112.2082].
- [25] R. Campanini, G. Ferri, and G. Ferri, *Phys. Lett.* **B703**, 237 (2011), [arXiv:1106.2008].
- [26] M. Csanád, T. Csörgö, Z.-F. Jiang, and C.-B. Yang, *Universe* **3**, 9 (2017) [arXiv:1609.07176].
- [27] J. Adam *et al.* [ALICE Collaboration], *Nature Phys.* **13**, 535 (2017) [arXiv:1606.07424].
- [28] A. Kurkela, A. Mazeliauskas, and R. Törnkvist, arXiv:2104.08179.

- [29] B.G. Zakharov, Phys. Rev. Lett. **112**, 032301 (2014) [arXiv:1307.3674].
- [30] B.G. Zakharov, J. Phys. G**41**, 075008 (2014) [arXiv:1311.1159].
- [31] S. Tripathy [for ALICE Collaboration], arXiv:2103.07218.
- [32] B.G. Zakharov, JETP Lett. **88**, 781 (2008) [arXiv:0811.0445].
- [33] B.G. Zakharov, JETP Lett. **80**, 617 (2004) [hep-ph/0410321].
- [34] B.G. Zakharov, JETP Lett. **112**, 681 (2020) [arXiv:2011.01526].
- [35] B.G. Zakharov, JETP Lett. **93**, 683 (2011) [arXiv:1105.2028].
- [36] B.G. Zakharov, JETP Lett. **103**, 363 (2016) [arXiv:1509.07020].
- [37] B.A. Kniehl, G. Kramer, and B. Potter, Nucl. Phys. B**582**, 514 (2000) [hep-ph/0010289].
- [38] T. Sjostrand, L. Lonnblad, S. Mrenna, and P. Skands, hep-ph/0308153.
- [39] R. Baier, Y.L. Dokshitzer, A.H. Mueller, and D. Schiff, JHEP **0109**, 033 (2001) [hep-ph/0106347].
- [40] B.G. Zakharov, JETP, **125**, 1071 (2017) [arXiv:1706.03980].
- [41] A. Bazavov *et al.*, Phys. Rev. D**98**, 054511 (2018) [arXiv:1804.10600].
- [42] J. Braun and H. Gies, Phys. Lett. B**645**, 53 (2007) [hep-ph/0512085].
- [43] A.C. Mattingly and P.M. Stevenson, Phys. Rev. D**49**, 437 (1994) [hep-ph/9307266].
- [44] Yu.L. Dokshitzer, V.A. Khoze, and S.I. Troyan, Phys. Rev. D**53**, 89 (1996) [hep-ph/9506425].
- [45] O. Kaczmarek and F. Zantow, Phys. Rev. D**71**, 114510 (2005) [hep-lat/0503017].
- [46] P. Lévai and U. Heinz, Phys. Rev. C**57**, 1879 (1998) [hep-ph/9710463].
- [47] S. Borsanyi, G. Endrodi, Z. Fodor, A. Jakovac, S.D. Katz, S. Krieg, C. Ratti, and K. K. Szabo, JHEP **1011**, 077 (2010) [arXiv:1007.2580].
- [48] J.D. Bjorken, Phys. Rev. D**27**, 140 (1983).
- [49] S. Kretzer, H.L. Lai, F. Olness, and W.K. Tung, Phys. Rev. D**69**, 114005 (2004) [hep-ph/0307022].
- [50] K.J. Eskola, H. Paukkunen, and C.A. Salgado, JHEP **0904**, 065 (2009) [arXiv:0902.4154].
- [51] R. Baier, D. Schiff, and B.G. Zakharov, Ann. Rev. Nucl. Part. Sci. **50**, 37 (2000) [hep-ph/0002198].
- [52] B.G. Zakharov, JETP Lett. **86**, 444 (2007) [arXiv:0708.0816].
- [53] G.-Y. Qin, J. Ruppert, C. Gale, S. Jeon, G.D. Moore, and M.G. Mustafa, Phys. Rev. Lett. **100**, 072301 (2008) [arXiv:0710.0605].
- [54] R. Baier, A.H. Mueller, and D. Schiff, Phys. Lett. B**649**, 147 (2007) [nucl-th/0612068].

- [55] B. Betz and M. Gyulassy, AIP Conf. Proc. **1701**, 060006 (2016); DOI: 10.1063/1.4938669.
- [56] J.-Y.Ollitrault, Eur. J. Phys. **29**, 275 (2008) [0708.2433].
- [57] B. Müller and K. Rajagopal, Eur. Phys. J. C**43**, 15 (2005) [hep-ph/0502174].
- [58] D. Kharzeev and M. Nardi, Phys. Lett. B**507**, 121 (2001) [nucl-th/0012025].
- [59] B.G. Zakharov, JETP **124**, 860 (2017) [arXiv:1611.05825].
- [60] B.G. Zakharov, Eur. Phys. J. C**78**, 427 (2018) [arXiv:1804.05405].
- [61] B.I. Abelev *et al.* [STAR Collaboration], Phys. Rev. C**79**, 034909 (2009) [arXiv:0808.2041].
- [62] K. Aamodt *et al.* [ALICE Collaboration], Phys. Rev. Lett. **106**, 032301 (2011) [arXiv:1012.1657].
- [63] J. Adam *et al.* [ALICE Collaboration], Phys. Rev. Lett. **116**, 222302 (2016), [arXiv:1512.06104].
- [64] S. Acharya *et al.* [ALICE Collaboration], Phys. Lett. B**790**, 35 (2019) [arXiv:1805.04432].
- [65] B. Alver, M. Baker, C. Loizides, and P. Steinberg, arXiv:0805.4411.
- [66] M. Rybczynski, G. Stefanek, W. Broniowski, and P. Bozek, Comput. Phys. Commun. **185**, 1759 (2014) [arXiv:1310.5475].
- [67] H. De Vries, C.W. De Jager, and C. De Vries, Atomic Data and Nuclear Data Tables **36**, 495 (1987).
- [68] J. Adams *et al.* [STAR Collaboration], Phys. Rev. C**71**, 044906 (2005) [nucl-ex/0411036].
- [69] J. Adam *et al.* [ALICE Collaboration], Phys. Rev. C**93**, 024905(2016) [arXiv:1507.06842].
- [70] R. Baier, Nucl. Phys. A**715**, 209 (2003) [hep-ph/0209038].
- [71] A. Bzdak, B. Schenke, P. Tribedy, and R. Venugopalan, Phys. Rev. C**87**, 064906 (2013) [arXiv:1304.3403].
- [72] B. Schenke, P. Tribedy, and R. Venugopalan, Phys. Rev. Lett. **108**, 252301 (2012), [arXiv:1202.6646].
- [73] L. McLerran, M. Praszalowicz, and B. Schenke, Nucl. Phys. A**916**, 210 (2013) [arXiv:1306.2350].
- [74] C. Albajar *et al.* [UA1 Collaboration], Nucl. Phys. B**335**, 261 (1990).
- [75] B. Abelev *et al.* [ALICE Collaboration], Phys. Lett. B**720**, 52 (2013) [arXiv:1208.2711].
- [76] G. Aad *et al.* [ATLAS Collaboration], JHEP **1509**, 050 (2015) [arXiv:1504.04337].

- [77] S. Chatrchyan *et al.* [CMS Collaboration], Eur. Phys. J. **C72**, 1945 (2012) [arXiv:1202.2554].
- [78] S. Acharya *et al.* [ALICE Collaboration], JHEP **1811**, 013 (2018) [arXiv:1802.09145].
- [79] The ATLAS collaboration, ATLAS-CONF-2017-012, <http://cds.cern.ch/record/2244824?ln=en>.
- [80] V. Khachatryan *et al.* [CMS Collaboration], JHEP **1704**, 039 (2017) [arXiv:1611.01664].
- [81] S. Acharya *et al.* [ALICE Collaboration], Phys. Lett. **B788**, 166 (2019) [arXiv:1805.04399].
- [82] The ATLAS collaboration, ATLAS-CONF-2018-007, <http://cds.cern.ch/record/2318588>.
- [83] A.M. Sirunyan *et al.* [CMS Collaboration], JHEP **1810**, 138 (2018) [arXiv:1809.00201].
- [84] A. Adare *et al.* [PHENIX Collaboration], Phys. Rev. **C87**, 034911 (2013) [arXiv:1208.2254].
- [85] B. Abelev *et al.* [ALICE Collaboration], Phys. Lett. **B719**, 18 (2013) [arXiv:1205.5761].
- [86] G. Aad *et al.* [ATLAS Collaboration], Phys. Lett. **B707**, 330 (2012) [arXiv:1108.6018].
- [87] S. Chatrchyan *et al.* [CMS Collaboration], Phys. Rev. Lett. **109**, 022301 (2012) [arXiv:1204.1850].
- [88] M. Aaboud *et al.* [ATLAS Collaboration], Eur. Phys. J. **C78**, 997 (2018) [arXiv:1808.03951].
- [89] A.M. Sirunyan *et al.* [CMS Collaboration], Phys. Lett. **B776**, 195 (2018) [arXiv:1702.00630].
- [90] S. Acharya *et al.* [ALICE Collaboration], JHEP **1811**, 013 (2018) [arXiv:1802.09145].
- [91] S. Acharya *et al.* [ALICE Collaboration], arXiv:2104.03116.
- [92] V. Khachatryan *et al.* [CMS Collaboration], JHEP **1704**, 039 (2017) [arXiv:1611.01664].